PHYSICAL REVIEW B **73**, 081202(R) (2006)

Dark excitons in Cu_2O crystals for two-photon coherence storage in semiconductors

Kosuke Yoshioka and Makoto Kuwata-Gonokami*
Department of Applied Physics, The University of Tokyo, and Solution Oriented Research for Science and Technology (SORST), JST, 7-3-1 Hongo, Bunkyo-ku, Tokyo 113-8656, Japan
(Received 19 January 2006; published 22 February 2006)

The two-photon coherence of infrared pulses is preserved for more than 250 ps by dark excitons in Cu_2O crystals. Taking into account the nonlocal electron-hole exchange interaction, 1*s* orthoexcitons are split into one bright exciton state that is quadrupole active and two dark exciton states that are two-photon active but one-photon inactive. Interference of cold dark exciton waves excited by a phase-locked pulse pair is observed with an almost perfect visibility and a beating pattern indicating and an energy splitting in the μeV range is seen. The long-lived two-photon coherence of dark excitons indicates their strong potential for coherence storage applications.

DOI: 10.1103/PhysRevB.73.081202 PACS number(s): 78.47.+p, 42.50.Gy, 42.50.Md

Preserving and controlling the quantum mechanical coherence of photons is a key technology for advanced ultrafast photonics and quantum information technology, including optical routing and quantum repeaters. Electromagnetically induced transparency (EIT) (Ref. 1) of coherently driven ultracold atomic ensembles or repumped rare-earth ions in dielectrics is a very promising scheme for lossless photon manipulation, where a drastic reduction of the light group velocity[2,3] and a quantum memory of photons[4] have been realized. The heart of this phase preserving control of photons is the destructive quantum interference based on metastable states with a long-lived two-photon coherence. However in order to exclude incoherent processes, it is necessary to use dilute systems in which the oscillator strength is small. Atomic gases and repumped rare-earth ions in dielectrics with densities around 10^{13} (Ref. 2) and 10^{15} cm^{-3} (Refs. 3 and 5), respectively, have been used in previous experiments.

To efficiently control photons, it is important to find a condensed matter system where all the valence electrons are involved in the optical transitions so that light-matter interaction is strong. In particular, the formation of excitons leads to an enhanced dipole moment strengthening light-matter interaction. In usual cases, however, intrinsic and extrinsic effects rapidly destroy the phase-coherence of photoexcited states in condensed matter. One possible method to preserve the phase coherence in a solid is to store the phase information of photons into an ensemble of cold excitons that are decoupled from the radiation field. In this paper, we report on the observation of long-term preservation of two-photon coherence in the form of cold dark excitons in bulk Cu_2O, which is a typical semiconductor system.

The yellow series exciton states in centrosymmetric Cu_2O consists of a 4*s*-like conduction electron and a 3*d*-like valence hole combined to form hydrogenlike envelope functions and are known as the most typical example of Wannier-Mott excitons in semiconductors. The fourfold 1*s* exciton states split into threefold degenerate orthoexciton states with a higher energy and a lower, nondegenerate paraexciton state by electron-hole exchange interaction. In the 1*s* orthoexcitons under investigation electric dipole transitions are forbidden, whereas electric quadrupole interactions are weakly optically active. Moreover, two-photon dipole transitions are allowed. Due to these selection rules, resonant second harmonic emission can occur in this centrosymmetric system as for *s*-*d* transitions in alkali atoms[6] but with enhanced efficiency.

In crystalline solids, which possess translation symmetry, all electronic states are indexed by a wave vector **K**. The electron-hole exchange interaction has a small but finite **K**-dependent component due to the nonlocal character of the interaction so that the threefold degeneracy of orthoexciton states $|O_{yz}\rangle$, $|O_{zx}\rangle$, and $|O_{xy}\rangle$ is lifted for nonzero **K** states. Recent high-resolution linear absorption spectroscopy revealed a fine splitting of the order of a few μeV.[7] The orientation-dependent selection rules for one-photon quadrupole transitions is discussed in Ref. 8.

We revisited the optical selection rules[9,10] to find the condition to selectively excite "dark" exciton states without generating "bright" excitons. Figure 1(a) schematically illustrates the overall optical configuration for the experiments we performed, which is a typical example of such a selective excitation of dark exciton states. The excitation beam is set parallel to the [110] crystal axis. In this configuration two dark exciton states, $|O_1\rangle=(-|O_{yz}\rangle+|O_{zx}\rangle)/\sqrt{2}$ and $|O_3\rangle=|O_{xy}\rangle$, and one bright exciton state, $|O_2\rangle=(|O_{yz}\rangle+|O_{zx}\rangle)/\sqrt{2}$, are obtained. For the dark exciton states one-photon transitions are forbidden, but two-photon dipole transitions are allowed. For the bright exciton state, only one-photon quadrupole transitions are allowed and two-photon transitions are forbidden. Table I shows a detailed description of these selection rules. Due to this complementarity, coherent resonant second-harmonic emission processes are inhibited. Thus, the emission from the bright exciton state $|O_2\rangle$ should occur via incoherent repopulation processes from the coherent dark exciton states $|O_1\rangle$ and $|O_3\rangle$. As a result, upon photoexcitation of the dark states, the quadrupole emission has a finite rise time. Such a fine splitting of 1*s* orthoexcitons should affect time-resolved stimulated two-photon emission[11] and second harmonic generation.[12,13]

The experiments are performed with high-quality natural single Cu_2O crystal samples with 440 and 800 μm thicknesses that are cooled down to 1.8 K in a liquid helium cryostat and held in a nearly strain-free state. Figure 1(b) shows the result of emission measurements under resonant two-photon excitation with nearly transform-limited 2 ps pulses,

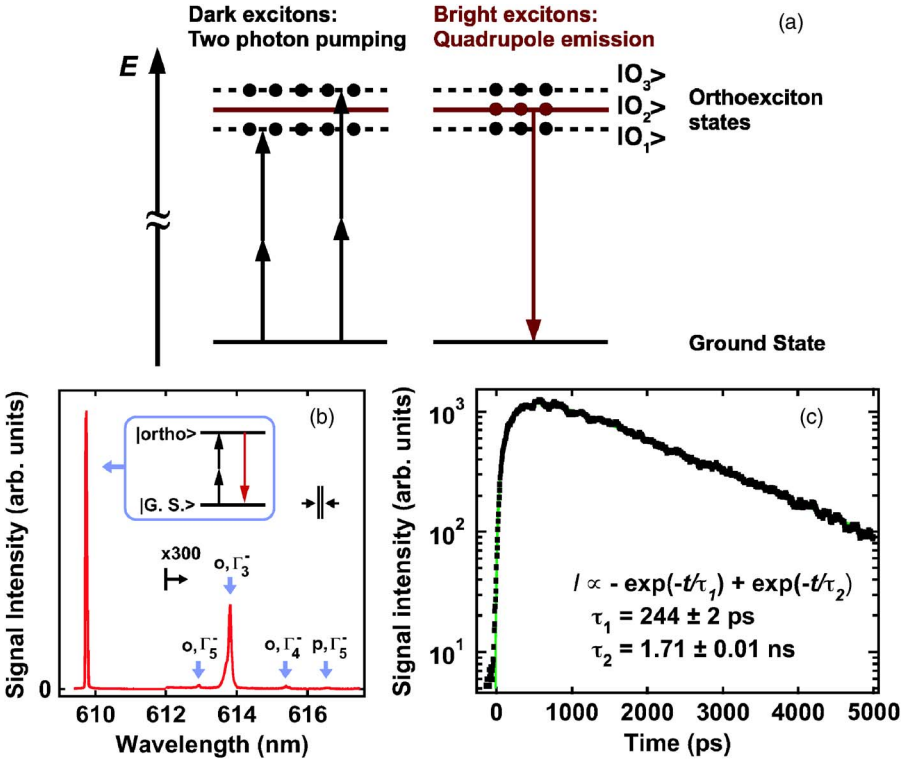

FIG. 1. (Color online) (a) Orthoexciton energy levels and optical transitions for $\mathbf{K}\|[110]$. The initial exciton population relaxes to a uniform distribution among the three states [black and red (dark gray) circles]. (b) Time-integrated photoluminescence spectrum under two-photon resonant excitation of $1s$ orthoexcitons in a 440-μm-thick Cu_2O crystal at 1.8 K. The four lines in the right part (300× magnified) are the phonon-assisted luminescence of ortho (o) and para (p) excitons, which are not discussed here. (c) Time-resolved two-photon resonant emission (609.74 nm) at 1.8 K, detected by a synchroscan streak camera. A double-exponential fit [green (gray) solid curve] convoluted with a 40 ps resolution was done to obtain a 244±2 ps rise time and a 1.71±0.01 ns fall time.

centered at 1219.5 nm (repetition rate: 76 MHz). The wave vector of the pump beam is parallel to the [110] crystal axis. We observe a very narrow resonant emission line at orthoexciton resonance ($\lambda=609.74$ nm), as was reported in previous work for different crystal orientations.[12–14] We performed a time-resolved measurement of this line using a synchroscan streak camera with a 40 ps time resolution. The temporal evolution, Fig. 1(c), shows a finite rise time of 244 ps (followed by a long decay time of 1.7 ns), in strong contrast with the case of coherent second harmonic generation (SHG) where the pulsed signal closely follows the excitation pulse. This implies that orthoexciton levels are split into bright and dark exciton states as discussed above.

The fact that the dark exciton states $|O_1\rangle$ and $|O_3\rangle$ are decoupled from the radiation field implies that they can store phase information of photons in a form of two-photon coherence for a long time. To measure this coherence time, we performed a coherent optical control experiment[15,16] of the population of dark excitons. The experimental setup is shown in Fig. 2(a). A sequence of phase-locked laser pulse pairs is obtained using a Michelson interferometer, and the two-photon resonant quadrupole emission intensity is measured as a function of the pulse separation time. The excitation power density is 6.1 MW/cm^2, and the resulting estimated initial orthoexciton density per pulse is 2.5×10^{11} cm^{-3}. This density (mean interexciton distance of 1 μm) can be considered a low density limit since the exciton Bohr radius is smaller than 1 nm.[17]

The lower part of Fig. 2(b) shows the optical interference pattern of the two pump pulses having a central wavelength $\lambda_p=1219.5$ nm when they fully overlap each other in time. We observe an oscillation period $\Delta\tau=(c/\lambda_p)^{-1}=4.07$ fs, where c is the velocity of light. We next separate the pump-pulse pair by a coarse delay $\tau_c=8.0$ ps, which is longer than the 2.0 ps pulse duration, and vary the fine pulse interval τ_f. We observe an interference pattern with almost perfect contrast (94% visibility), oscillating with a period of 2.03 fs, which is half that of the pump pulse as shown in the upper part of Fig. 2(b). This is evidence that the phase coherent ensembles of dark excitons are created via two-photon absorption of pulses and behave as macroscopic quantum waves to preserve two-photon coherence.[18] With τ_f corresponding to the minima in the interference pattern, two coherent dark exciton waves destructively interfere and most of the generated population vanishes.

The dephasing time of the coherent dark exciton waves was directly measured by observing the maxima and minima of the interference patterns as a function of the coarse delay (τ_c), and the first-order field autocorrelation functions of dark exciton waves were thus obtained. According to the two-photon polarization selection rules (Table I), the ratio of the transition rate to the two dark exciton states is given by $N_1:N_3=\sin^2 2\theta:\sin^4\theta$, where N_1 and N_3 are the number of

TABLE I. One-photon and two-photon polarization selection rules for three eigenstates with $\mathbf{K}\|[110]$. $W^{(1)}$ and $W^{(2)}$ denote the one-photon and two-photon transition rates, respectively. θ is the linear polarization angle of the excitation light relative to the [001] crystal axis. One can see that the population ratio between the $|O_1\rangle$ and $|O_3\rangle$ dark exciton states can be tuned by rotating the pump polarization.

Eigenstate	$W^{(1)}$	$W^{(2)}$
$\|O_1\rangle$	0	$\propto \sin^2 2\theta$
$\|O_2\rangle$	$\propto \cos^2\theta$	0
$\|O_3\rangle$	0	$\propto \sin^4\theta$

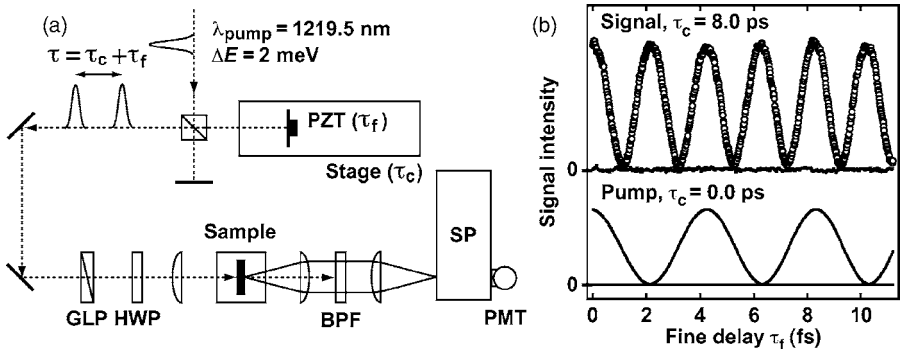

FIG. 2. (a) Experimental setup. The coarse time delay τ_c between two excitation pulses is obtained by using a mechanical motorized stage. The fine delay τ_f controlling the relative optical phase between the two pulses is obtained by precisely tuning the voltage applied to a piezoelectric transducer (PZT). The orientation of the linear polarization plane of the pump beam is controlled with a Glan laser prism (GLP) and a half wave plate (HWP). The time-integrated resonant emission signal is dispersed with a spectrometer (SP) and detected with a photomultiplier (PMT). A band pass filter (BPF) cuts the pump beam. (b) (Upper part) Resonant emission intensity of orthoexcitons as a function of τ_f. (τ_c=8.0 ps) for T=1.7 K. (Lower part) An interference pattern of the optical pump pulses observed for τ_c=0.0 ps. The linear polarization of the excitation light is set 45° relative to the [001] crystal axis.

created dark excitons in the states $|O_1\rangle$ and $|O_3\rangle$. When we set θ=50°, we maximize the total efficiency of two-photon excitation of both the $|O_1\rangle$ and $|O_3\rangle$ states (the same condition as in time-resolved measurement of Fig. 1). We observe a clear beating signal with a decay time over 200 ps [Fig. 3(a)], which originates from the quantum beat of excitons with fine structures. A further proof is obtained when θ is set to 90° and we find that the $|O_3\rangle$ state is predominantly excited so that the beat is suppressed as shown in Fig. 3(b).

The dark exciton wave is the coherent superposition of the $|O_1\rangle$ and $|O_3\rangle$ states with eigenenergies E_1 and E_3. The phase-space compression scheme of pulsed two-photon excitation[18] enables us to excite excitons into very narrow energy distributions. We can describe the wave function of dark excitons coherently driven by pulsed two-photon excitation with the ith pulse at t=0 as $|\phi^{(i)}(t)\rangle = c_1 \exp[-i(E_1/\hbar)t - t/T_d]|O_1\rangle + c_3 \exp[-i(E_3/\hbar)t - t/T_d + \delta]|O_3\rangle$, where δ is the relative phase between the two

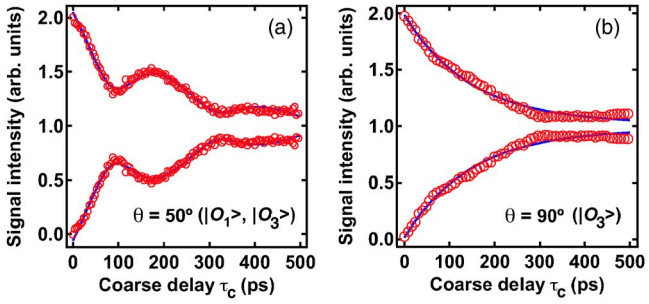

FIG. 3. (Color online) First-order autocorrelation functions of dark exciton waves at T=1.7 K: maxima and minima of the interference pattern as a function of the coarse delay (open circles). Each maximum and minimum is normalized with respect to the average of the two. (a) θ=50° (both $|O_1\rangle$ and $|O_3\rangle$ are excited). The solid curve is a theoretical fit (see text). (b) θ=90° (only the state $|O_3\rangle$ is initially populated). The signal intensity is about half as high as in (a) and therefore a lower signal-to-noise ratio is obtained. The solid curve is a theoretical fit with an exponential function. A small deviation from a single exponential decay can be due to a local strain.

pure states, and we assumed the same lifetime T_d for both components. The total wave function generated by the double pulses (i=1,2) separated from each other by a delay $\tau=\tau_c+\tau_f$, is the sum of the wave functions, $|\Psi(t,\tau)\rangle = |\phi^{(1)}(t)\rangle + |\phi^{(2)}(t-\tau)\rangle$. The quadrupole emission signal I_{sig} from the bright exciton state we detected is proportional to the square amplitude of the total exciton waves, that is, $I_{sig} \propto \int_0^\infty \langle\Psi(t,\tau)|\Psi(t,\tau)\rangle dt$. We performed a least-squares curve fit of the data in Fig. 3(a) with the above equation and were able to reproduce the curves to obtain the dephasing time, energy splitting, and ratio of created population between $|O_1\rangle$ and $|O_3\rangle$. The estimated lower limit of the dephasing time of dark excitons, from the measured T_d of I_{sig}, is 235±10 ps, which corresponds to a dephasing rate of $\Gamma_d = 2\hbar/T_d$ = 5.60±0.24 μeV. Such a long dephasing time is comparable to the ones of one-exciton states in single quantum dots.[19,20] The rise time 244±2 ps of the quadrupole emission signal shown in Fig. 1(c), which could be a measure of the longitudinal relaxation of dark excitons, is about twice as long as expected from T_d. This implies that inelastic processes such as repopulation from dark excitons to the dark and bright exciton states, and elastic pure dephasing processes, have a comparable contribution to the dephasing of dark excitons. We obtain an energy splitting between the dark exciton levels $\Delta_{31}=E_3-E_1$=17.8±0.2 μeV, which is about four times larger than the value obtained by off-angle beam one-photon absorption measurements.[7] This discrepancy can be explained by the small but finite residual strain of the natural crystals, especially along the [110] axis, that have not been perfectly removed by annealing. The obtained population ratio is $N_3/N_1 = c_3^2/c_1^2$=0.349±0.015, which is in good agreement with the calculated ratio $\sin^4(50°)/\sin^2(2\times 50°)$ =0.355. This result clearly indicates that the two dark exciton sublevels are well separated at low temperature and proves the arguments of the selection rules. The fit gives a relative phase offset δ=0.698±0.056 rad.

To clarify the mechanism of the dephasing of dark excitons, we performed temperature dependence measurements. We observe the linear dependence of the dephasing rate on

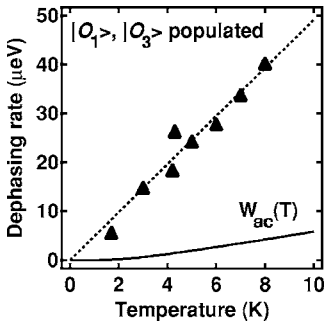

FIG. 4. (Closed triangles) Dephasing rate of coherent dark excitons as a function of lattice temperature. These values are extracted from the autocorrelation functions measured at each temperature. The excitation pulses are linearly polarized with $\theta=50°$ relative to the crystal [001] axis as in Fig. 3(a). (Dotted line) Theoretical fit by a linear function, taking zero dephasing at zero temperature. (Solid curve) Calculated dephasing rate for 1*s* orthoexcitons assuming an intraband acoustic-phonon scattering process. The temperature-dependent spectral broadening $W_{ac}(T)$ is given by $W_{ac}(T)=2g_{ex}k_BT_1/\pi[\exp(T_1/T)-1]$, where T_1 is defined as $T_1=2m_{ex}u^2/k_B$; $m_{ex}=2.7m_e$ (m_e: electron mass) (Ref. 21), $u=4.5\times10^5$ cm/s, and k_B are the effective mass of an orthoexciton, sound velocity in the crystal, and Boltzmann constant, respectively. The orthoexciton-acoustic-phonon coupling constant g_{ex} is given by $g_{ex}=(m_{ex}E_d)^2/\hbar^3\rho u$ (ρ: densit y of the crystal), and $E_d=1.8$ eV (Ref. 22) is the deformation potential for orthoexcitons.

temperature as shown in Fig. 4. Such a linear dependence in the low temperature region could be ascribed to intraband single acoustic-phonon scattering, which sets the fundamental limit of coherence time of dark excitons. The calculation (solid curve), however, returns much smaller dephasing rates than the experimental ones. This indicates that the observed dephasing of the dark excitons is dominated by other incoherent processes including repopulation among the three orthoexciton states. It also implies that we can prolong the coherence storage time up to the fundamental limit, the order of 10 ns [dephasing rate of 0.4 μeV (100 MHz)] at 2 K, by a careful tuning of the exciton levels obtained by applying a magnetic field or a uniaxial stress to suppress the repopulation. We note that the coherence measurement we have shown cannot remove temperature-independent inhomogeneous broadening due to random local strain.

It is interesting to reconsider the excitonic EIT scheme mentioned in Ref. 23. Here we propose to use a dark orthoexciton state as a "metastable state" in a lambda-type three-level system. The combination of the long-lived two-photon coherence of dark exciton states and strong dipole coupling of the $1s$-np ($n=2,3,\cdots$) transitions assures a well-established, broadband EIT window in the np absorption band (of a few meV bandwidth) and a strong induced dispersion to decrease the group velocity of light pulses.

In conclusion, we have found that dark exciton states in a bulk Cu_2O crystal can preserve two-photon coherence over 250 ps by two-photon coherent control experiments. Such a long-lived two-photon coherence in a high-density system in solid state media is essential for efficient and lossless phase-preserving photon manipulations using intrinsic electronic states in condensed matter.

We thank J. B. Héroux for critical reading of the manuscript. This work is partly supported by the Grant-in-Aid for Scientific Research (S) from Japan Society for the Promotion of Science (JSPS).

*Electronic address: gonokami@ap.t.u-tokyo.ac.jp

[1] S. E. Harris, Phys. Today **50** (7), 36 (1997).
[2] L. V. Hau, S. E. Harris, Z. Dutton, and C. H. Behroozi, Nature (London) **397**, 594 (1999).
[3] A. V. Turukhin, V. S. Sudarshanam, M. S. Shahriar, J. A. Musser, B. S. Ham, and P. R. Hemmer, Phys. Rev. Lett. **88**, 023602 (2002).
[4] D. F. Phillips, A. Fleischhauer, A. Mair, R. L. Walsworth, and M. D. Lukin, Phys. Rev. Lett. **86**, 783 (2001).
[5] E. Kuznetsova, O. Kocharovskaya, P. Hemmer, and M. O. Scully, Phys. Rev. A **66**, 063802 (2002).
[6] D. S. Bethune, R. W. Smith, and Y. R. Shen, Phys. Rev. Lett. **37**, 431 (1976).
[7] G. Dasbach, D. Fröhlich, H. Stolz, R. Klieber, D. Suter, and M. Bayer, Phys. Rev. Lett. **91**, 107401 (2003).
[8] G. Dasbach, D. Fröhlich, R. Klieber, D. Suter, M. Bayer, and H. Stolz, Phys. Rev. B **70**, 045206 (2004).
[9] R. J. Elliot, Phys. Rev. **124**, 340 (1961).
[10] M. Inoue and Y. Toyozawa, J. Phys. Soc. Jpn. **20**, 363 (1965).
[11] D. Fröhlich, K. Reimann, and R. Wille, Europhys. Lett. **3**, 853 (1987); K. Reimann and R. Wille, J. Lumin. **38**, 60 (1987).
[12] S. Kono, N. Naka, M. Hasuo, S. Saito, T. Suemoto, and N. Nagasawa, Solid State Commun. **97**, 455 (1996).
[13] M. Y. Shen, S. Koyama, M. Saito, T. Goto, and N. Kuroda, Phys. Rev. B **53**, 13477 (1996).
[14] Y. Sun, G. K. L. Wong, and J. B. Ketterson, Phys. Rev. B **63**, 125323(R) (2001).
[15] A. P. Heberle, J. J. Baumberg, and K. Köhler, Phys. Rev. Lett. **75**, 2598 (1995).
[16] N. H. Bonadeo, J. Erland, D. Gammon, D. Park, D. S. Katzer, and D. G. Steel, Science **282**, 1473 (1998).
[17] T. Tayagaki, A. Mysyrowicz, and M. Kuwata-Gonokami, J. Phys. Soc. Jpn. **74**, 1423 (2005).
[18] M. Kuwata-Gonokami, R. Shimano, and A. Mysyrowicz, J. Phys. Soc. Jpn. **71**, 1257 (2002).
[19] D. Birkedal, K. Leosson, and J. M. Hvam, Phys. Rev. Lett. **87**, 227401 (2001).
[20] P. Borri, W. Langbein, S. Schneider, U. Woggon, R. L. Sellin, D. Ouyang, and D. Bimberg, Phys. Rev. Lett. **87**, 157401 (2001).
[21] P. Y. Yu and Y. R. Shen, Phys. Rev. B **12**, 1377 (1975).
[22] D. W. Snoke, D. Braun, and M. Cardona, Phys. Rev. B **44**, 2991 (1991).
[23] M. Artoni, G. C. La Rocca, and F. Bassani, Europhys. Lett. **49**, 445 (2000).